For $TCID_{50}$-infectivity assays, GL37 cell monolayers in 96-well cell culture plates were incubated with 50 µl of serially diluted mAb2 for 1 h at 37°C in a CO_2 incubator. Without washing, 25 µl of HAV, genotype IA, IB or IIIB, was added to the appropriate wells and incubated for 1 h at 37°C. Cells were infected with all HAVs at a multiplicity of infection of 100. Infected cells were maintained in Eagle's minimal essential medium (EMEM) supplemented with 2 mM L-glutamine, 50 µg/ml of gentamicin, 2% fetal bovine serum and 0.15% of sodium bicarbonate (2% FBS-EMEM) for 3 days. Infected cells were fixed with 80% methanol containing 0.03% H_2O_2, and air-dried, and then HAV propagated in infected cells was detected using anti-HAV hyperimmune rabbit serum. The plates were washed and incubated with HRPO anti-rabbit IgG (MBL, Nagoya, Japan), and then the rate of blocking of infection was measured using the formula:

Blocking rate (%) = 100 × (absorbance without inhibitor − absorbance with inhibitor)/absorbance without inhibitor.

The immunofocus assay was a modified radioimmunofocus assay [13] as follows: We mixed 50 µl of mAb2 (diluted 1:20 in PBS supplemented with 2% FBS) with an equal volume of HAV, genotype IA, IB or IIIB, containing 40–60 focus-forming units (FFU) in 2% FBS-EMEM. GL37 cell monolayers in six-well cell culture plates (Falcon, Franklin Lakes, NJ, USA) were inoculated with 100 µl of the mAb2-HAV mixture and incubated for 1 h at 37°C in a 5% CO_2 environment to allow mAb2 and virus adsorption to the cells. Without removing the inoculum, the GL37 monolayer was overlaid with 5 ml of Dulbecco's modified Eagle medium (Nissui, Tokyo, Japan) containing 0.6% agarose ME (Iwai Chemicals Company, Tokyo, Japan), 2% FBS and 0.22% sodium bicarbonate. After the agar had solidified, the cultures were placed upside down and incubated at 37°C for 10–12 days at 37°C in 5% CO_2. The agarose overlay was discarded, and the cells were fixed with 1.5 ml of 80% methanol containing 0.03% H_2O_2 for 1 h at 4°C. Anti-HAV rabbit hyperimmune serum (1 ml of 1:2,000 dilution) was added to each well and incubated overnight at 4°C. The wells were washed with PBS and then incubated with 1 ml of HRPO anti-rabbit IgG for 2 h at 37°C. The plates were washed once again, and then HAV foci were detected using 1.5 ml of DAB substrate [0.5 mg/ml diaminobenzidine, 0.03% $(NH_4)_2Ni(SO_4)_2$, 0.03% $CoCl_2$, 0.03% H_2O_2 in PBS]. Infection was considered blocked if the input FFU was reduced by $\geq$50%.

Results

Binding properties of mAb2s

Among the hybridoma clones secreting mAb2, two stable clones were selected by KF94-binding ELISA. The ascitic fluids of the selected clones, designated mAb2 94-2 and 94-7 were specific for KF94, and they did not react with either KF6 or HAV-negative human serum. The titers of mAb2 94-2 and 94-7, given as the reciprocal of the endpoint dilution required to generate maximal absorbance in KF94-binding ELISA, were 102,400 and 25,600, respectively. Both were categorized as IgG1 subclass, κ chain. They did not cross-react or bind to HAV.

Interactions between mAb2s, KF94 and HAV

Figure 1a shows that both mAb2s inhibited KF94 binding to HAV. At a 1:1,000 dilution, mAb2 94-2 and 94-7

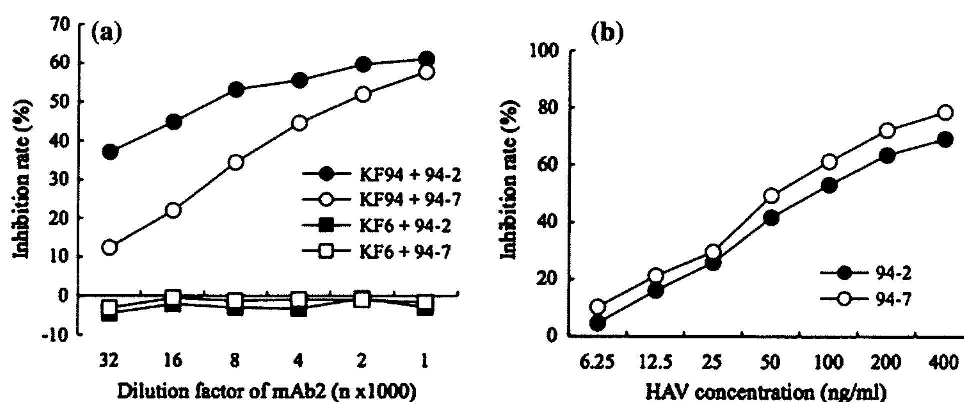

Fig. 1 Interactions between KF94, mAb2s and HAV. Anti-HAV antibodies KF6 and KF94 were incubated with serially diluted mAb2 94-2 or 94-7 (*filled circle*, KF94 and 94-2; *open circle*, KF94 and 94-7; *filled square*, KF6 and 94-2; *open square*, KF6 and 94-7; (**a**), and then binding to inactivated HAV was determined by ELISA. The mAb2s (diluted 1:1,000) inhibited KF94 binding to HAV by 60%. The mAb2s did not interfere with KF6 binding to HAV, thus confirming their specificity. Anti-HAV antibody KF94 was incubated with serially diluted inactivated HAV, and binding of preincubated KF94 to mAb2 94-2 (*filled circle*) or 94-7 (*open circle*) was determined by ELISA. Inactivated HAV interfered with mAb2 binding to KF94 (**b**)

inhibited 61.1 and 57.7% of the binding, respectively, and the inhibition rate gradually decreased with higher dilutions. The inhibition ability was specific for KF94. The mAb2s did not affect anti-HAV human mAb KF6 binding to HAV.

Inactivated HAV inhibited KF94 binding to mAb2s (Fig. 1b). The inhibition rates were proportional to the concentration of inactivated HAV. KF94 binding to the mAb2s 94-2 and 94-7 was inhibited by 69.1 and 78.5%, respectively, at the maximal concentration of inactivated HAV. Binding of mAb2s or HAV to KF94 reduced the affinity of KF94.

Binding of mAb2 to HAV cellular receptor

Binding of mAb2 94-7 and anti-HAV receptor antibodies 190/4, 235/4, and 263/6 to GL37 cells was confirmed by immunofluorescence staining (Fig. 2). Neither mAb2 94-2 nor NMS bound to GL37 cells.

We performed competitive inhibition ELISA to confirm that mAb2 94-7 and anti-HAV receptor antibody shared the same HAV cellular receptor. Anti-HAV receptor antibody 235/4 and mAb2 94-7 competed with the HRPO anti-HAV receptor 190/4C for binding to HAV cellular receptors. Figure 3 shows that the inhibition rates were proportional to the concentrations of the competitors. At a 1:100 dilution, the inhibition rates of the positive competitor, mAb2 94-7 and 94-2, and the negative competitor were 93.2, 59.2, 20.8 and 18.5%, respectively. The inhibition rate of mAb2 94-7 was lower than that of the anti-HAV-receptor antibody 235/4, but higher than that of the mAb2 94-2 or the negative competitor.

MAb2-mediated protection of GL37 cells from HAV infection

The rates of mAb2 94-7-mediated blocking of GL37 cell infection with HAV in $TCID_{50}$-infectivity assays were 65.8, 54.1, and 86.0% for genotypes IA, IB, and IIIB, respectively. Blocking rates are expressed as dose-response curves (Fig. 4). On the other hand, mAb2 94-2 enhanced HAV propagation rather than protecting the cells.

Immunofocus assays showed that the number of immunofoci of genotype IIIB strain KRM003 was reduced by 83.3% in the presence of mAb2 94-7 diluted 1:40. The results were similar for genotypes IA and IB, which reduced the number of immunofoci by 71.1 and 77.8%, respectively, at the same dilution. In contrast, mAb2 94-2 did not reduce the numbers of immunofoci.

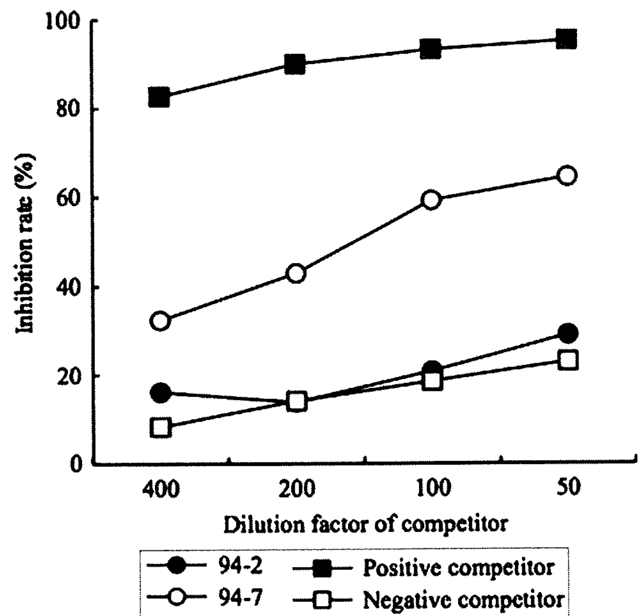

Fig. 3 Binding of mAb2s to GL37 cells in competition with anti-HAV receptor antibody. Positive competitor (*filled square*) and mAb2 94-7 (*open circle*) interfered with HRPO anti-receptor antibody 190/C binding to GL37 cells by recognizing the common HAV receptors of GL37 cells. The competitive inhibition rates of mAb2 94-2 (*filled circle*) and of negative competitor (*open square*) were equally low

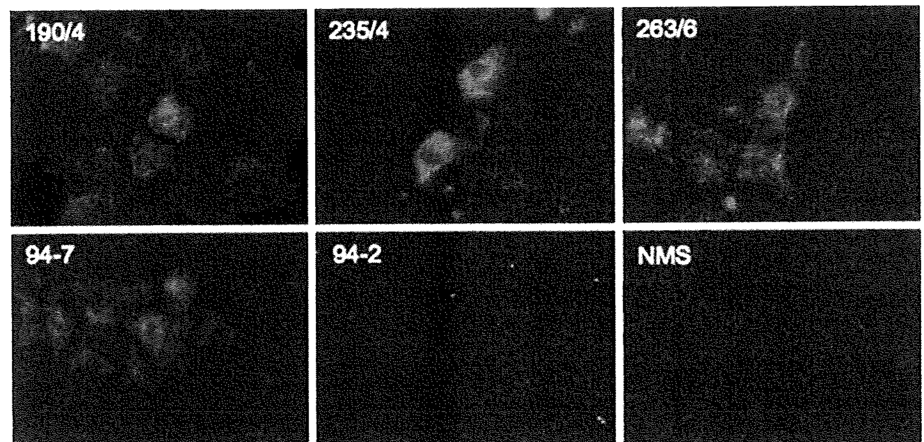

Fig. 2 Binding of mAb2s to GL37 cells. MAb2 94-7 and anti-receptor antibodies (190/4, 235/4 and 263/6) bound to GL37 cells were detected by immunofluorescence assay. MAb2 94-2 and normal mouse serum (*NMS*) were undetectable

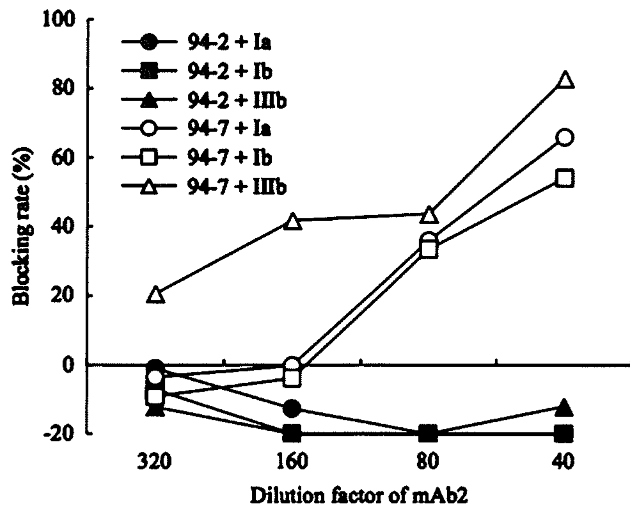

Fig. 4 MAb2-mediated protection of GL37 cells from HAV infection determined by $TCID_{50}$-infectivity assay. GL37 cells were protected from HAV infection by mAb2 94-7, but not by mAb2 94-2. Combinations of mAb2 and HAV genotypes: *filled circle* 94-2 and IA; *filled square* 94-2 and IB; *filled triangle*, 94-2 and IIIB; *open circle*, 94-7 and IA; *open square*, 94-7 and IB; *open triangle*, 94-7 and IIIB

Discussion

We generated the anti-idiotypic antibodies mAb2 94-2 and 94-7 by immunizing a mouse with anti-HAV neutralizing antibody KF94. The mAb2s were specific for the parental anti-HAV antibody KF94 and did not cross-react. They inhibited the binding of KF94 to HAV (Fig. 1a), and inactivated HAV competitively inhibited the binding of KF94 to the mAb2s (Fig. 1b), suggesting that the mAb2s and HAV bound to the paratope of KF94. Each mAb2 recognized different idiotopes within the paratope and could bind to KF94 as a surrogate of HAV.

These data indicated that the mAb2s mimic an HAV neutralization site that is complementary to the paratope of KF94. However, mimicry of the neutralization site by mAb2s might be incomplete, because the mAb2s inhibited KF94-HAV binding by only about 60%.

The characteristics of the mAb2s differed with respect to their affinity for the HAV-susceptible cell line GL37. The mAb2 94-2 neither bound to GL37 cells (Fig. 2) nor inhibited HAV infection (Fig. 4). The mAb2 94-2 seemed to have mimicked a portion of the antibody-binding site in the HAV neutralization site. The mimicked antibody-binding site interfered with KF94-HAV binding but did not influence virus-cellular receptor interaction.

On the other hand, mAb2 94-7 competed with the anti-HAV-cellular-receptor antibodies for binding to GL37 cells (Figs. 2, 3). The binding of mAb2 94-7 to GL37 cells partially blocked HAV infection (Fig. 4). We postulate that the mAb2 94-7 mimicked the part of the neutralization site that contains functional antibody-binding and cellular-receptor-binding sites.

The speculation that mimicry of the HAV neutralization site by mAb2 would be incomplete also explains why mAb2 94-7 could not totally block HAV infection. MAb2 94-7 was capable of blocking the infectivity of different genotypic strains (Fig. 4) and thus seems to mimic a common receptor-binding site among genotypes IA, IB and IIIB. Thus, these genotype strains might infect GL37 cells via a common receptor. Among the three genotypes, the rate at which mAb2 94-7 blocked infection was highest against strain IIIB (Fig. 4), which might be because KF94 was prepared from a patient infected with HAV strain IIIB.

Anti-idiotypic antibodies induced by immunization with an anti-Sindbis-virus neutralizing antibody competed with the virus for cellular receptors [22]. This suggested that a crucial receptor-binding site exposed on the viral surface is recognized by Ab1. We also speculate that the HAV receptor-binding site is exposed on the viral surface, because mAb2 94-7 competed with HAV for cellular receptors. Furthermore, the syngeneic mAb2 94-2 mimics part of the antibody-binding site. These data indicate that the antibody- and receptor-binding sites mimicked by mAb2s are exposed on the viral surface and are in close vicinity or overlap, thus comprising an epitope that could induce KF94.

Unlike other members of the family *Picornaviridae* [3], very little is understood about HAV neutralization sites and relationships between antibody- and receptor-binding sites. However, all published data support the notion that major and minor immunodominant neutralization sites exist on HAV virions and empty capsids [17, 19]. The immunodominant neutralization sites of native particles appear to be conformational and generally differ from those of denatured particles or isolated HAV structural proteins. Antibodies elicited by immunization with native or formalin-inactivated virus have broad neutralizing activity against different strains [20]. In contrast, the development of neutralizing antibodies in response to individual structural proteins, synthetic peptides, or expressed uncleaved precursors and polypeptides is problematic [7, 10, 15]. Thus, analysis of HAV neutralization sites using such probes is not simple. Analysis of HAV neutralization sites has mainly depended on the use of neutralization-escape mutants generated by serial passage of the virus in cultured cells in the presence of neutralizing mouse monoclonal antibodies [17, 19]. Although HAV strains isolated from various parts of the world belong to a single serotype [18], neutralization-escape mutants can be produced experimentally. These mutants are expected to possess a replicative advantage and survive more efficiently than wild-type virus as a result of the arrangement of surface neutralizing antibody-binding sites. However,

their in vivo replication is restricted compared with wild-type virus, although they appear to be equally stable in vitro [14]. Furthermore, although the rate of substitution throughout the HAV genome is high, most of the mutations are silent [6]. Presumably, alterations in neutralizing-antibody-binding sites, such as in neutralization-escape mutants, might arise during natural infection. However, constraints probably prevent this from occurring in nature. Our results indicated that one such constraint depends on the relationship between antibody- and receptor-binding sites on the viral surface. These sites might be closely located or overlap within an immunodominant neutralization site. Therefore, mutations on the antibody-binding site might result in deterioration of the receptor-binding site. Such deterioration would consequently reduce the affinity of the HAV receptor-binding site, which would result in neutralization escape mutants being unable to replicate to significant levels in vivo. Alterations in antibody-binding sites of poliovirus are thought to be responsible for the affinity of the receptor-binding site [8]. The relationship between the antibody- and receptor-binding sites shown by mAb2s might partly explain why only one serotype of HAV exists.

To our knowledge, we are the first to analyze the HAV surface using anti-Ids to mimic receptor- and antibody-binding sites within HAV neutralizing sites. Our anti-Ids could not completely mimic the viral surface structure, but they remained functionally intact. Anti-Id antibodies may be considered obsolete, but they nevertheless represent an effective tool with which to structurally analyze the viral surface.

Acknowledgments The authors would like to thank Dr. Hiroshi Yamamoto and Dr. Yasuo Moritsugu for important suggestions regarding this study.

References

1. Bona CA (1998) Idiotype vaccines: forgotten but not gone. Nat Med 4:668–669
2. Bona CA, Kohler H (1984) Anti-idiotypic antibodies and internal images. In: Venter JC, Fraser CM, Lindstrom J (eds) Monoclonal and anti-idiotypic antibodies: probes for receptor structure and function. Alan R Liss inc, New York, pp 141–149
3. Che Z, Olson NH, Leippe D et al (1998) Antibody-mediated neutralization of human rhinovirus 14 explored by means of cryoelectron microscopy and X-ray crystallography of virus-Fab complexes. J Virol 72:4610–4622
4. Chiba J (1988) A strategy for the production of human monoclonal antibodies. Hum Cell 1:31–36
5. Coulepis AG, Locarnini SA, Gust ID (1980) Iodination of hepatitis A virus reveals a fourth structural polypeptide. J Virol 35:572–574
6. Garcia-Aguirre L, Cristina J (2008) Analysis of the full-length genome of hepatitis A virus isolated in South America: heterogeneity and evolutionary constraints. Arch Virol 153:1473–1478
7. Gauss-Muller V, Deinhardt F (1988) Immunoreactivity of human and rabbit antisera to hepatitis A virus. J Med Virol 24:219–228
8. Harber J, Bernhardt G, Lu H-H et al (1995) Canyon rim residues, including antigenic determinants, modulate serotype-specific binding of polioviruses to mutants of the poliovirus receptor. Virology 214:559–570
9. Hiernaux JR (1988) Idiotypic vaccines and infectious diseases. Infect Immun 56:1407–1413
10. Hughes JV, Stanton LW (1979) Isolation and immunizations with hepatitis A viral structural proteins: induction of antiprotein, antiviral, and neutralizing responses. J Virol 55:395–401
11. Kaplan G, Totsuka A, Thompson P et al (1996) Identification of a surface glycoprotein on African green monkey kidney cells as a receptor for hepatitis A virus. EMBO J 15:4282–4296
12. Kiyohara T, Satoh T, Totsuka A et al (2007) Shifting seroepidemiology of hepatitis A in Japan, 1973–2003. Microbiol Immunol 51:185–191
13. Lemon SM, Binn LN, Marchwicki RH (1983) Radioimmunofocus assay for quantitation of hepatitis A virus in cell cultures. J Clin Microbiol 17:834–839
14. Lemon SM, Binn LN, Marchwicki R et al (1990) In vivo replication and reversion to wild type of a neutralization-resistant antigenic variant of hepatitis A. J Infect Dis 161:7–13
15. Mattioli S, Imberti L, Stellini R et al (1995) Mimicry of the immunodominant conformation-dependent antigenic site of hepatitis A virus by motifs selected from synthetic peptide libraries. J Virol 69:5294–5299
16. Melnick JL (1995) History and epidemiology of hepatitis A virus. J Infect Dis 171(Suppl 1):s2–s8
17. Ping L-H, Lemon SM (1992) Antigenic structure of human hepatitis A virus defined by analysis of escape mutants selected against murine monoclonal antibodies. J Virol 66:2208–2216
18. Robertson BH, Jansen RW, Khanna B et al (1992) Genetic relatedness of hepatitis A virus strains recovered from different geographical regions. J Gen Virol 73:1365–1377
19. Stapleton JT, Lemon SM (1987) Neutralization escape mutants define a dominant immunologic neutralization site on hepatitis A virus. J Virol 61:491–498
20. Totsuka A, Moritsugu Y (1994) Hepatitis A vaccine development in Japan. In: Nishioka K, Suzuki H, Mishiro S et al (eds) Viral hepatitis and liver disease. Springer, Tokyo, pp 509–513
21. Uytdehaag FGCM, Bunschoten H, Ket Weijer et al (1986) From Jenner to Jerne: towards idiotype vaccines. Immunol Rev 90:93–113
22. Wang K-S, Schmalgohn AL, Kuhn RG et al (1991) Antiidiotypic antibodies as probes for the Sindbis virus receptor. Virology 181:694–697

ELSEVIER

Journal of Hepatology 50 (2009) 883–894

Journal of Hepatology

www.elsevier.com/locate/jhep

HCV replication suppresses cellular glucose uptake through down-regulation of cell surface expression of glucose transporters☆

Daisuke Kasai[1,†], Tetsuya Adachi[1,†], Lin Deng[1], Motoko Nagano-Fujii[1], Kiyonao Sada[1], Masanori Ikeda[2], Nobuyuki Kato[2], Yoshi-Hiro Ide[1], Ikuo Shoji[1], Hak Hotta[1,*]

[1]*Divisions of Microbiology, Kobe University Graduate School of Medicine, 7-5-1 Kusunoki-cho, Chuo-ku, Kobe 650-0017, Japan*
[2]*Department of Molecular Biology, Okayama University Graduate School of Medicine and Dentistry, Okayama, Japan*

See Editorial, pages 845–847

Background/Aims: **Persistent infection with hepatitis C virus (HCV) causes extrahepatic diseases, including diabetes. We investigated the possible effect(s) of HCV replication on cellular glucose uptake and expression of the facilitative glucose transporter (GLUT) 2 and 1.**

Methods: **We used Huh-7.5 cells harboring either an HCV subgenomic RNA replicon (SGR) or an HCV full-genomic RNA replicon (FGR), HCV-infected cells, and the respective cells treated with interferon (IFN). We also used liver tissue samples obtained from patients with or without HCV infection.**

Results: **Glucose uptake and surface expression of GLUT2 and GLUT1 were suppressed in SGR, FGR and HCV-infected cells compared to the control cells. Expression levels of GLUT2 mRNA, but not GLUT1 mRNA, were lower in SGR, FGR and HCV-infected cells than in the control. Luciferase reporter assay demonstrated decreased GLUT2 promoter activities in SGR, FGR and HCV-infected cells. IFN treatment restored glucose uptake, GLUT2 surface expression, GLUT2 mRNA expression and GLUT2 promoter activities. Also, GLUT2 expression was reduced in hepatocytes of liver tissues obtained from HCV-infected patients.**

Conclusions: **HCV replication down-regulates cell surface expression of GLUT2 partly at the transcriptional level, and possibly at the intracellular trafficking level as suggested for GLUT1, thereby lowering glucose uptake by hepatocytes.**
© 2009 European Association for the Study of the Liver. Published by Elsevier B.V. All rights reserved.

Keywords: **Diabetes mellitus; Down-regulation; Glucose uptake; GLUT1; GLUT2; Hepatitis C virus; Hepatocyte; Interferon; Replicon**

1. Introduction

Hepatitis C virus (HCV) is a small, enveloped RNA virus, which belongs to the genus *Hepacivirus* within the family *Flaviviridae*. The viral genome consists of single-stranded, positive-sense RNA of 9.6 kb that encodes a polyprotein of about 3000 amino acids. There are six major genotypes of HCV worldwide, with each genotype being further classified into a number of subtypes, such as HCV-1a and -1b [1,2]. The polyprotein is processed by host cellular and viral proteases to yield at least 10 structural and nonstructural (NS) proteins, such

Received 15 June 2008; received in revised form 19 November 2008; accepted 11 December 2008; available online 27 February 2009
Associate Editor: F. Zoulim

☆ The authors who have taken part in the research of this manuscript declared that they do not have a relationship with the manufacturers of the materials involved either in the past or present and they did not receive funding from the manufacturers to carry out their research.

* Corresponding author. Tel.: +81 78 3825500; fax: +81 78 3825519.
E-mail address: hotta@kobe-u.ac.jp (H. Hotta).
† These authors contributed equally to this work.

Abbreviations: FGR, full-genome RNA replicon; GLUT, glucose transporter; HBV, hepatitis B virus; HCV, hepatitis C virus; IFN, interferon; SGR, subgenomic RNA replicon.

0168-8278/$36.00 © 2009 European Association for the Study of the Liver. Published by Elsevier B.V. All rights reserved.
doi:10.1016/j.jhep.2008.12.029

as core protein, envelope glycoproteins (E1 and E2), p7, NS2, NS3, NS4A, NS4B, NS5A and NS5B [3,4].

HCV prevails in most parts of the world with an estimated number of about 170 million carriers and, hence, HCV infection is a major global healthcare problem [5]. Persistent infection with HCV causes not only liver diseases, including hepatitis, but also extrahepatic manifestations, such as type 2 diabetes [6–8]. While it has been known that liver cirrhosis impairs the glucose metabolism of the liver, there are some reports showing that HCV-infected patients over 40 years old have an increased risk for type 2 diabetes – three times higher than that for patients without HCV infection [9,10]. These reports imply the possibility that HCV infection directly predisposes the host towards type 2 diabetes. However, the precise mechanism(s) is poorly understood.

Glucose is transported into the cell via various isoforms of the facilitative glucose transporter (GLUT) that are present in most cells. Currently, a total of 14 isoforms have been identified in the GLUT family [11–13]. GLUT2 is expressed tissue-specifically in the liver, pancreatic β-cells, hypothalamic glial cells, retina and enterocytes [14]. On the other hand, GLUT1 is expressed at high levels in all fetal tissues and, in adults, it is widely expressed but most abundant in erythrocytes, endothelial cells of the blood–brain barrier, renal tubules of the kidney, and any kind of malignant cells including hepatocellular carcinoma [13].

In the present study, we demonstrated that HCV infection suppressed hepatocytic glucose uptake through down-regulation of surface expression of GLUT in a human hepatocellular carcinoma-derived cell line Huh-7.5. We also demonstrated that GLUT2 expression in hepatocytes of the liver tissues from HCV-infected patients was lower than in those from patients without HCV infection. We propose that HCV replication decreases glucose uptake and cell surface expression of GLUT, which would eventually lead to glucose metabolism disorder.

2. Materials and methods

2.1. Cell culture, HCV RNA replication, HCV infection and IFN treatment

A human hepatoma-derived cell line, Huh-7.5, which is highly permissive to HCV RNA replication [15], was kindly provided by Dr. C.M. Rice (The Rockefeller University, New York, NY, USA). The cells were maintained in Dulbecco's modified Eagle's medium supplemented with 10% heat-inactivated fetal calf serum.

Huh-7.5 cells stably harboring an HCV-1b subgenomic RNA replicon (referred to as SGR cells, hereafter) were prepared as describe previously [16–18], using pFK5B/2884Gly (a kind gift from Dr. R. Bartenschlager, University of Heidelberg, Heidelberg, Germany). In SGR cells, the HCV subgenomic RNA replicon autonomously replicates to express NS3 to NS5B of HCV (Fig. 1). Cells harboring a full-length HCV-1b RNA replicon derived from pON/C-5B (referred to as FGR cells, hereafter) were described previously [19,20]. In FGR cells, the genome-size HCV RNA replicon autonomously replicates to express all the HCV proteins (the core protein, E1, E2, p7, NS2, NS3 to NS5B).

The pFL-J6/JFH1 plasmid that encodes the entire viral genome of a chimeric strain of HCV-2a, J6/JFH1 [21], was kindly provided by Dr. C.M. Rice. The HCV RNA genome was transcribed *in vitro* from pFL-J6/JFH1 and transfected to Huh-7.5 cells. The virus produced in the culture supernatant was used for infection experiments at multiplicities of infection of 1.0 and cultured for 5 days after virus infection.

In some experiments, SGR and FGR cells, as well as HCV-infected cells at 5 days after virus infection, were treated with 1000 IU/ml of IFN (Sigma, St. Louis, MI, USA) for 10 days to eliminate HCV replication.

2.2. Immunofluorescence

Cells were fixed with 3.7% paraformaldehyde and incubated with mouse monoclonal antibody against HCV NS5A (Chemicon International, Inc., Temecula, CA, USA) or HCV core (Abcam, Tokyo, Japan). The cells were then incubated with fluorescein isothiocyanate (FITC)-conjugated goat anti-mouse IgG (MBL Co. Ltd., Nagoya, Japan), and observed under a fluorescent microscope (BX51; Olympus, Tokyo, Japan).

2.3. Immunoblotting

Cells were solubilized in lysis buffer as reported previously [22]. The cell lysates were electrophoresed subjected to 8% polyacrylamide gel electrophoresis and transferred to polyvinylidene difluoride membrane (Millipore Corp., Billerica, MA, USA). The membranes were incubated with mouse monoclonal antibodies against HCV NS5A or NS3 (Chemicon), followed by incubation with peroxidase-conjugated goat anti-mouse IgG (MBL). The positive bands were visualized by using ECL detection system (GE Healthcare UK Ltd., Buckinghamshire, UK).

2.4. Uptake of 2-deoxy-D-glucose and thymidine

Cells cultured in 12-well plates were deprived of serum by incubation in serum-free medium for 12 h. The cells were then pre-incubated for 20 min in 450 μl of KRH (25 mM Hepes, 120 mM NaCl, 5 mM KCl, 1.2 mM $MgSO_4$, 1.3 mM $CaCl_2$, 1.3 mM KH_2PO_4 and 0.1% BSA, pH 7.4). Glucose uptake assay was performed as describe previously [23]. In brief, glucose uptake was initiated by addition of 50 μl of reaction solution (KRH containing 0.5 mM, 0.25 μCi 2-deoxy-D-[1,2-^{3}H]glucose) to each well. As a negative control, 100 μM phloretin was added to reaction solution. After 10 min, transport was terminated by washing the cells with ice-cold KRH buffer containing 100 μM phloretin. The cells were solubilized by 0.1% sodium dodecyl sulfate, and the incorporated radioactivity was measured by liquid scintillation counter (LS6500; Beckman Coulter, Fullerton, CA). In some experiments, GLUT1 and GLUT2 were ectopically expressed by using the pCAGGS expression vector [24] and glucose uptake was measured as described above.

2.5. Flow cytometry

To examine cell surface expression of GLUT1 and GLUT2, cells harvested in PBS containing 0.2% EDTA were incubated with rabbit polyclonal antibodies against GLUT1 or GLUT2 (1:200; Alpha Diagnostic International, San Antonio, TX, USA) on ice for 1 h. After being washed, the cells were incubated with FITC-labeled goat anti-rabbit IgG (1:200; BD Pharmingen, Franklin Lakes, NJ, USA) on ice for another 1 h. Analysis was carried out using flow cytometer and a total of 10,000 live cell events were measured. Results were displayed graphically as overlaying histograms demonstrating the shift of the mean FITC staining value.

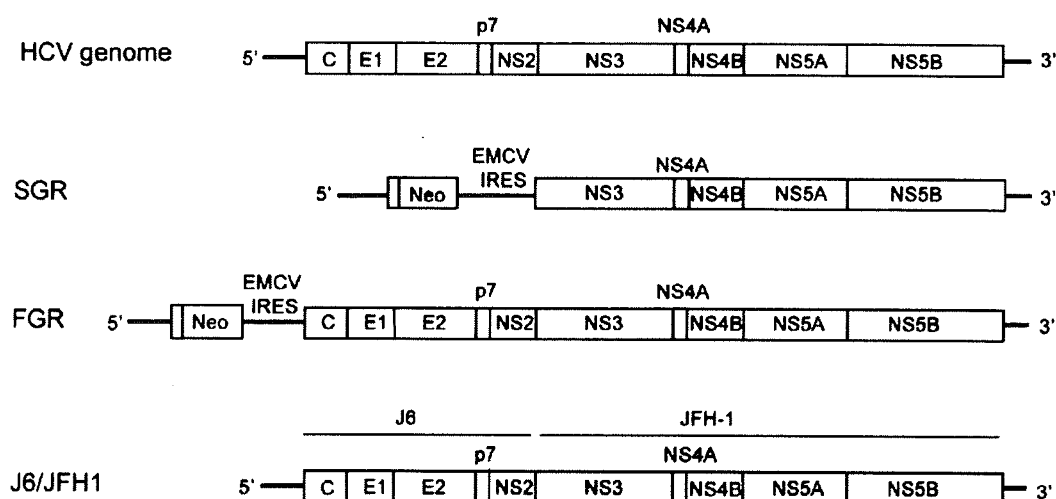

Fig. 1. The HCV genome and HCV RNA replicons. Schematic diagram of the HCV genome, SGR, FGR and the chimeric HCV J6/JFH1 genome are shown. EMCV IRES, encephalomyocarditis virus internal ribosome entry site; Neo, neomycin-resistance gene.

2.6. Real-time quantitative RT-PCR

Total cellular RNA was isolated using the TRIzol reagent (Invitrogen Corp., Carlsbad, CA, USA) and cDNA was generated using QuantiTect Reverse Transcription system (Qiagen, Valencia, CA, USA). Real-time quantitative PCR was performed on a SYBR *Premix Ex Taq* (Takara Bio, Kyoto, Japan) using SYBR green chemistry in ABI PRISM 7000 (Applied Biosystems, Foster, CA, USA). β-Glucuronidase was used as an internal control. The primers used are shown in Table 1.

2.7. Luciferase reporter assay

We constructed the human GLUT2 promoter-luciferase reporter gene (pGLUT2-1291Luc) by cloning a 1.6-kb genomic fragment that encompasses the human GLUT2 promoter (−1291 to +308) [14] into the pGL4 vector plasmid (Promega, Madison, WI, USA). pGLUT2-1291Luc thus contains a 1291-bp fragment of the human GLUT2 promoter upstream of the minimal promoter and the coding sequence of the *Photinus pyralis* (firefly) luciferase. pRL-CMV-*Renilla* (Promega) was used as an internal control. Cells were transfected with pGLUT2-1291Luc (1 μg) and pRL-CMV-*Renilla* (10 ng). After 24 h, a luciferase assay was performed by using Dual-luciferase reporter assay system (Promega). Firefly and *Renilla* luciferase activities were measured by Lumat LB 9501 (Berthold, Bad Wildbad, Germany). Firefly luciferase activity was normalized to *Renilla* luciferase activity for each sample.

2.8. Immunohistochemistry

Human adult liver autopsy materials and surgically removed liver tissues of patients with HCV- or HBV-associated hepatocellular carcinoma, and those with metastatic liver cancer were obtained with written informed consent. The tissues were fixed with 10% buffered formalin (pH 7.0), embedded in paraffin and sectioned at intervals of 4 μm. Immunohistochemical staining was performed with a DAKO ENVISION+ Kit (Dako, Glostrup, Denmark). In brief, fixed sections were treated with 3% hydrogen peroxide, and were autoclaved at 121 °C for 20 min. Then, the sections were incubated with a blocking solution and then with either anti-GLUT2 rabbit polyclonal antibody (Santa Cruz Biotechnology, Santa Cruz, CA, USA) or normal rabbit IgG (Santa Cruz Biotechnology) as a control. The sections were incubated with horseradish peroxidase-labeled polymer-conjugated goat anti-rabbit IgG, followed by incubation in a chromogenic solution. The sections were then counterstained with hematoxylin and examined with a light microscope. GLUT2 expression levels were arbitrarily determined by two examiners, including a pathologist, in a blinded manner.

2.9. Statistical analysis

Results were expressed as mean ± SEM. Statistical significance was evaluated by ANOVA, and statistical significance was defined as $P < 0.05$.

Table 1
Sequences and positions of the primers used in this study.

Gene name (GenBank ID)	Primer	Position	PCR product (bp)
GLUT2	5′-TGGGCTGAGGAAGAGACTGT-3′	279–298	461
(J03810)	5′-AGAGACTGAAGGATGGCTCG-3′	739–720	
GLUT1	5′-TGAACCTGCTGGCCTTC-3′	437–453	399
(AK292791)	5′-GCAGCTTCTTTAGCACA-3′	835–819	
HCV NS5B	5′-ACCAAGCTCAAACTCACTCCA-3′	9191–9211	119
(AJ238799)	5′-AGCGGGGTCGGGCACGAGACA-3′	9309–9289	
β-glucuronidase	5′-ATCAAAAACGCAGAAAATACG-3′	1747–1767	238
(M15182)	5′-ACGCAGGTGGTATCAGTCTTG-3′	1984–1964	

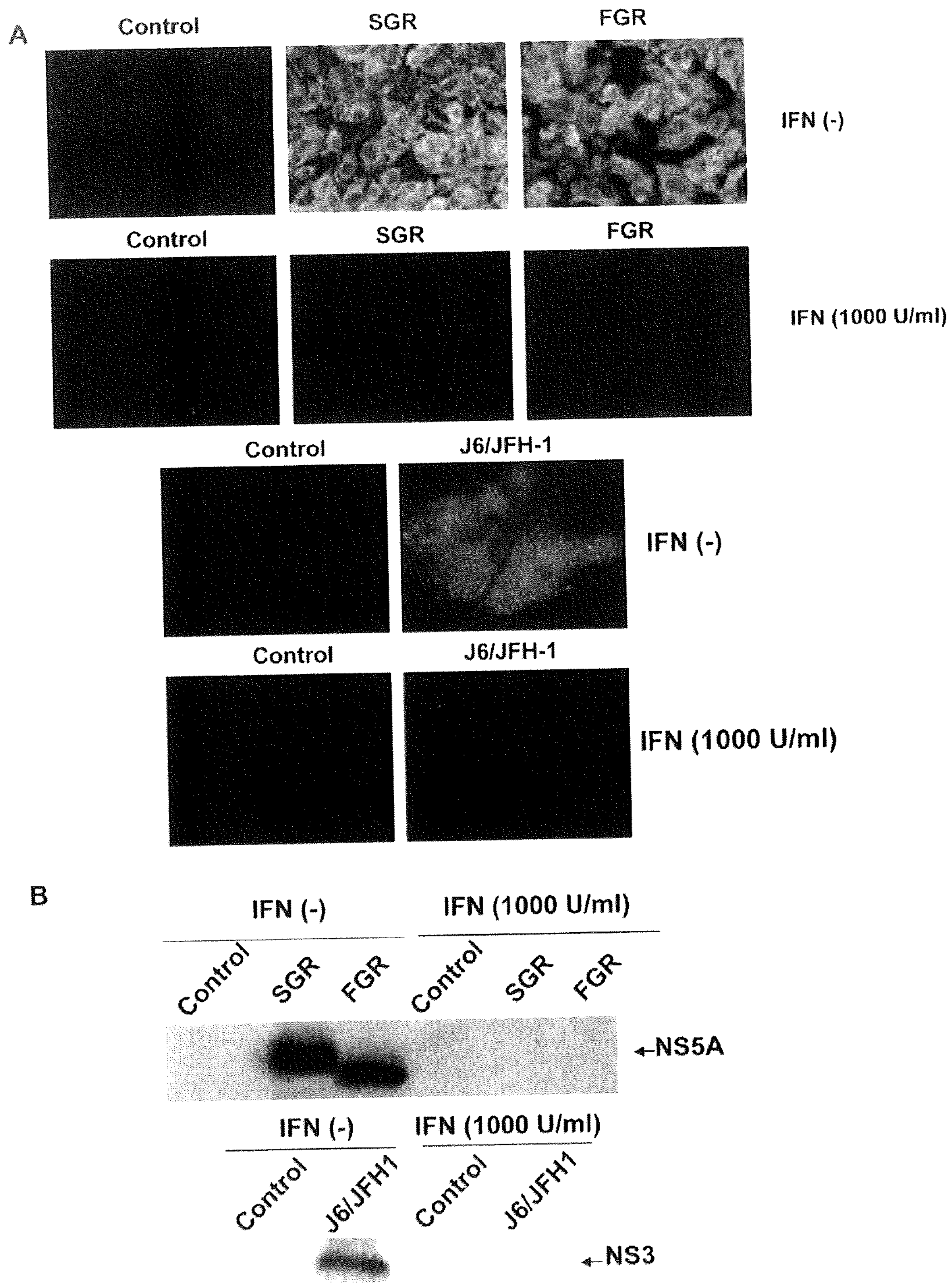

Fig. 2. Expression of HCV proteins in SGR, FGR, HCV-infected cells and the respective cells treated with IFN. (A) Cells were immunostained with anti-NS5A antibody (for SGR, FGR and the control cells) or anti-core antibody (for HCV-infected cells and the control). In parallel, cells were treated with IFN (1000 IU/ml) for 10 days to eliminate HCV replication before being subjected to immunostaining. (B) Cells were analyzed by immunoblotting with anti-NS5A antibody (upper panel) or anti-NS3 antibody (lower panel). In parallel, cells were treated with IFN (1,000 IU/ml) for 10 days to eliminate HCV replication before being subjected to immunoblotting.

3. Results

3.1. HCV protein expression in SGR, FGR, HCV-infected cells and those treated with IFN

Immunofluorescence analysis revealed that almost all the cells in SGR and FGR cultures, and >90% of the cells in the HCV J6/JFH1-infected culture were positive for HCV antigens (Fig. 2A). Western blot analysis also confirmed HCV protein expression in SGR, FGR and HCV-infected cells (Fig. 2B). In some experiments, HCV replication in SGR, FGR and HCV-infected cells was eliminated by IFN treatment for 10 days (Fig. 2A and B).

3.2. Selective suppression of cellular glucose uptake by HCV replication

2-Deoxygluose uptake levels in SGR, FGR and HCV-infected cells were significantly suppressed by about 50–60%, compared with the control Huh-7.5 cells (Fig. 3A and B). On the other hand, thymidine uptake, which was used as a control, did not significantly differ among all the cells tested (data not shown). Moreover, glucose uptake levels in SGR, FGR and HCV-infected cells were restored by IFN treatment (Fig. 3A and B). These results strongly suggest that cellular glucose uptake is selectively suppressed by HCV RNA replication.

3.3. Down-regulation of cell surface expression of GLUT2 and GLUT1 by HCV replication

GLUT2 is the principal glucose transporter of hepatocytes *in vivo* while GLUT1 is expressed in a wide variety of cultured cells. We therefore examined cell surface expression of GLUT2 and GLUT1 by flow cytometry analysis. As shown in Fig. 4A, cell surface expression of GLUT2 and GLUT1 was markedly down-regulated in SGR and FGR cells, compared with the control. On the other hand, cell surface expression of transferrin receptor was not significantly suppressed in SGR or FGR, compared with the control, with the result ensuring the specificity of the down-regulation of GLUT2 and GLUT1 cell surface expression in SGR and FGR (Fig. 4A). Moreover, treatment of SGR and FGR cells with IFN restored the surface expression of GLUT2 and GLUT1 (Fig. 4A). These results suggest that HCV RNA replication specifically mediates down-regulation of GLUT2 and GLUT1.

Down-regulation of GLUT2 surface expression was observed also in HCV-infected cells (Fig. 4B). On the other hand, down-regulation of GLUT1 surface expression was only marginal and, compared to that of GLUT2, less evidently observed in HCV-infected cells. As a control, cell surface expression of transferrin receptor did not differ at all between HCV-infected cells and the control. Again, treatment of HCV-infected cells with IFN restored surface expression of GLUT2 (Fig. 4B).

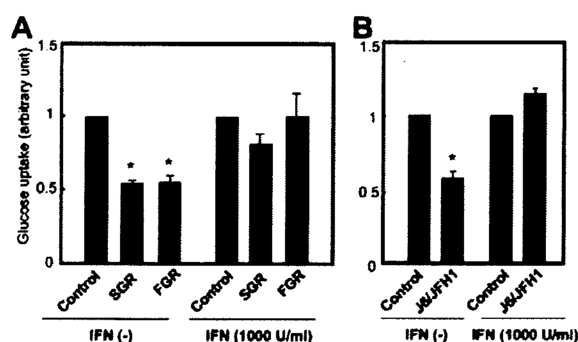

Fig. 3. Selective suppression of cellular glucose uptake by HCV replication. (A) Uptake of 2-deoxy-D-[1,2-^{3}H] glucose in SGR, FGR and HCV-negative control. In parallel, cells were treated with IFN (1000 IU/ml) for 10 days to eliminate HCV replication before being subjected to glucose uptake analysis. Data represent mean ± SEM of four independent experiments and the values for the control cells were arbitrarily expressed as 1.0. $^*P < 0.01$, compared with the control. (B) Uptake of 2-deoxy-D-[1,2-^{3}H] glucose in J6/JFH-1-infected cells and the uninfected control. In parallel, cells at 5 days after infection were treated with IFN (1000 IU/ml) for 10 days to eliminate HCV replication before being subjected to glucose uptake analysis.

3.4. Proteasomal degradation is not involved in the down-regulation of GLUT2 or GLUT1

Some viruses down-regulate cell surface molecules, such as immunoreceptors and intercellular adhesion molecules, through ubiquitination and proteasomal degradation of the target proteins [25]. To test this possibility, we treated SGR and FGR cells with lactacystin, a potent proteasome inhibitor. While lactacystin treatment enhanced cell surface expression of transferrin receptor, the same treatment did not increase cell surface expression of GLUT2 or GLUT1 in SGR or FGR cells (Fig. 5). This result suggested that down-regulation of cell surface expression of GLUT2 or GLUT1 in HCV-replicating cells was not due to increased degradation through the ubiquitin–proteasome system. The result rather implied the possible involvement of another mechanism(s), e.g., transcriptional suppression and/or impaired intracellular trafficking.

3.5. Transcriptional suppression of GLUT2, but not GLUT1, by HCV replication

To examine whether HCV RNA replication suppresses GLUT2 and GLUT1 expression at the transcriptional level, we measured mRNA expression levels by quantitative RT-PCR. The results obtained revealed that GLUT2 mRNA levels were reduced significantly in SGR, FGR and HCV-infected cells, compared to the control (Fig. 6A). It should be noted that the degree of GLUT2 mRNA suppression was greater in FGR

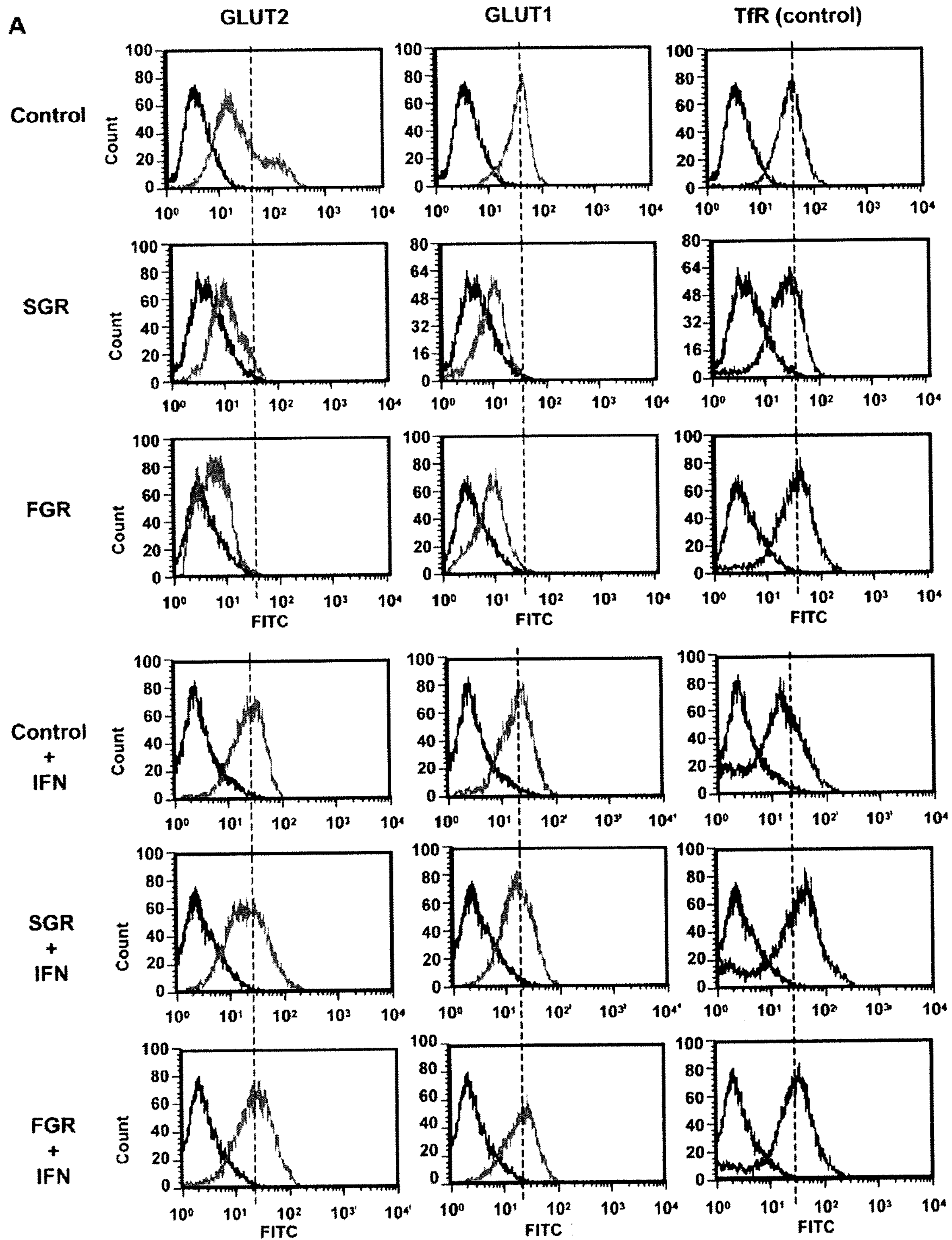

Fig. 4. Down-regulation of cell surface expressions of GLUT2 and GLUT1 by HCV replication. (A) SGR, FGR, the HCV-negative control cells were stained with specific antibodies, followed by FITC-conjugated second antibody (GLUT2, red line; GLUT1, green line) or stained with FITC-conjugated antibody alone (black line). Transferrin receptor (TfR) served as a control (blue line). In parallel, cells were treated with IFN (1000 IU/ml) for 10 days to eliminate HCV replication before being subjected to flow cytometry. (B) HCV-infected cells and the uninfected control were analyzed by flow cytometry as in (A). In parallel, cells at 5 days after infection were treated with IFN (1000 IU/ml) for 10 days to eliminate HCV replication before being subjected to flow cytometry analysis.

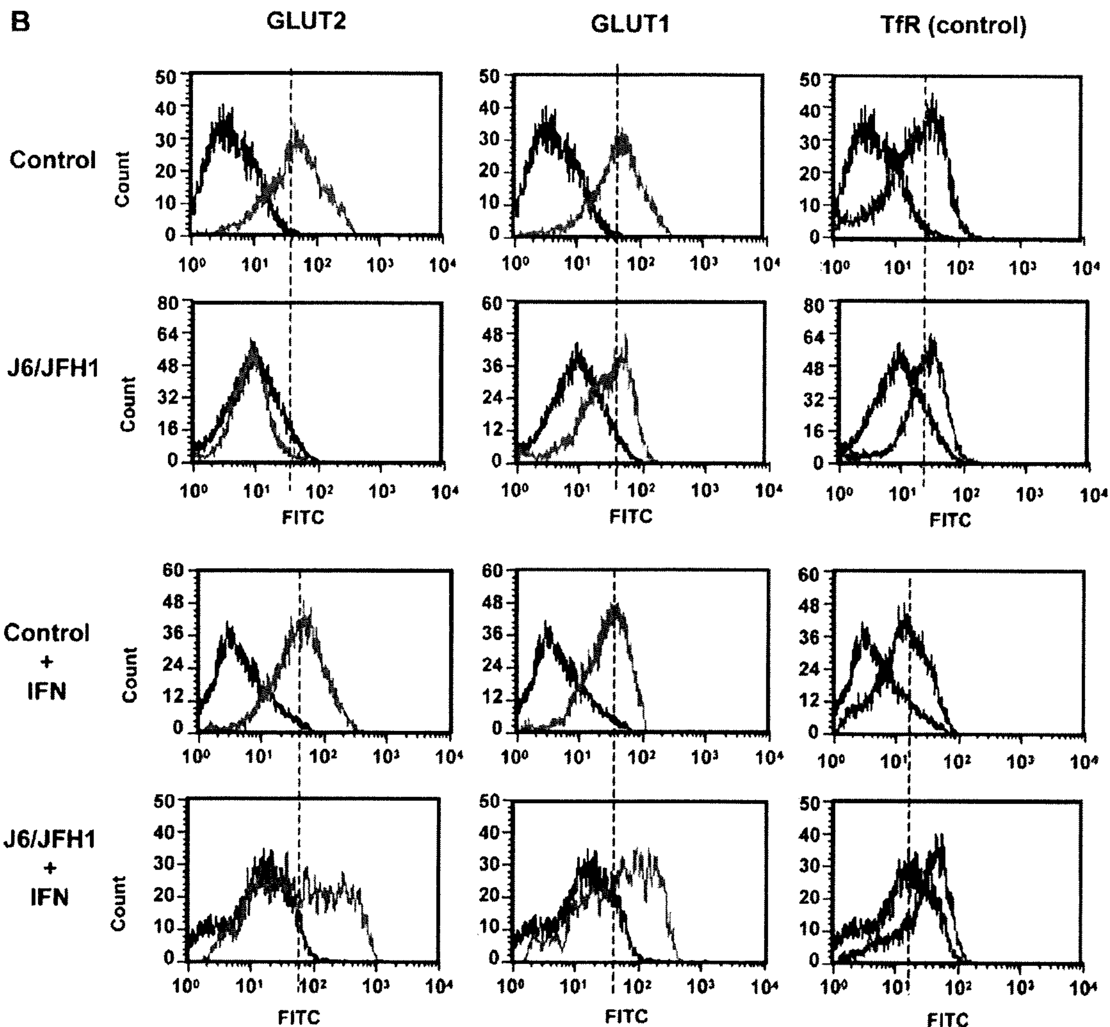

Fig. 4 (*continued*)

than in SGR cells. On the other hand, GLUT1 mRNA levels were not affected by HCV RNA replication (SGR and FGR) or HCV infection (Fig. 6B).

We also confirmed that GLUT2 mRNA expression levels in SGR, FGR and HCV-infected cells were restored by IFN treatment (Fig. 6A).

3.6. Suppression of GLUT2 promoter activity by HCV replication

Next, we performed luciferase reporter assay to examine the possible effect of HCV replication on GLUT2 promoter activities. The result obtained demonstrated that GLUT2 promoter activities were significantly suppressed in SGR, FGR and HCV-infected cells, compared to the control cells (Fig. 6C). Furthermore, GLUT2 promoter activities in SGR, FGR and HCV-infected cells were restored by IFN treatment. It is thus likely that HCV replication suppresses GLUT2 promoter activity, thereby decreasing GLUT2 mRNA levels.

3.7. Ectopically expressed GLUT1 or GLUT2 mediates increased glucose uptake in SGR, FGR and HCV-infected cells

We examined the possible effects of ectopically expressed GLUT1 and GLUT2 on glucose uptake in SGR, FGR and HCV-infected cells. Glucose uptake was significantly increased by ectopically expressed GLUT1 or GLUT2 in SGR, FGR and HCV-infected cells as well as in the control Huh-7.5 cells (Fig. 6D). It should be noted that, in this series of transient transfection experiments, only ca. 20% of the cells were ectopically overexpressing GLUT1 or GLUT2. These results collectively suggest the possibility that down-regulation

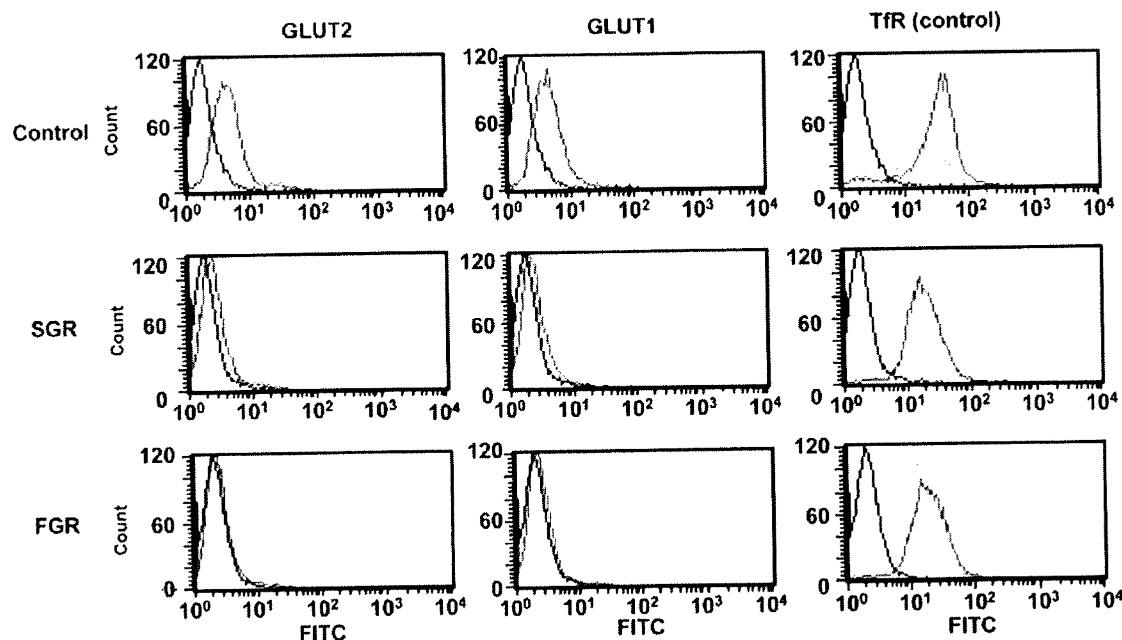

Fig. 5. Effects of lactacystin treatment on cell surface expression of GLUT2, GLUT1 and transferrin receptor (TfR). Cells were treated with lactacystin (10 μM) overnight to inhibit proteasomal degradation, and analyzed by flow cytometry. Cells treated with lactacystin are shown in red line and those left untreated in blue line. The negative controls stained with FITC-conjugated antibody alone are shown in black line.

of GLUT1 and GLUT2 expression is primarily involved in the decreased glucose uptake in SGR, FGR and HCV-infected cells.

3.8. Decreased GLUT2 expression in hepatocytes obtained from HCV-infected patients

GLUT2 is the principal glucose transporter expressed in hepatocytes *in vivo*. As shown in Fig. 7B, practically all hepatocytes obtained from patients without HCV infection showed positive staining for GLUT2, which was most evidently observed near the plasma membrane. On the other hand, hepatocytes obtained from HCV-infected patients showed markedly reduced GLUT2 staining in most, if not the entire, areas of the section, compared with the uninfected control (Fig. 7D). This heterogeneous staining pattern might reflect concomitant presence of areas comprising either virus-infected or uninfected hepatocytes in a tissue sample. Whereas all the sections obtained from 8 patients without HCV infection showed evenly positive staining for GLUT2, sections from 8 (89%) of 9 HCV-infected patients showed moderately to markedly reduced GLUT2 staining (Table 2). Reduced GLUT2 staining was observed also with hepatocytes in the liver tissues obtained from HBV-infected patients. However, the areas of reduced GLUT2 staining appeared to be more restricted in sections obtained from HBV-infected patients than in those from HCV-infected ones.

4. Discussion

HCV infection is known as an initiation and precipitating factor of type 2 diabetes [7–10,26,27]. Progression of liver fibrosis induced by persistent viral infection may induce diabetes [28]. Furthermore, it has been reported that the prevalence of diabetes is higher among patients with HCV-associated liver cirrhosis than in those with HBV-associated cirrhosis [7]. It is likely, therefore, that HCV infection itself is a risk factor of diabetes. Previous reports suggest that HCV infection directly causes insulin resistance that would cause the progression of diabetes [29–31]. However, the underlying mechanism(s) is not yet completely elucidated. In this study, we analyzed the effect of HCV infection on cellular glucose uptake and expression of glucose transporters.

We observed that glucose uptake was suppressed in cells harboring HCV RNA replicons (SGR and FGR) and those infected with HCV than in the control cells (Fig. 3). It has been reported that glucose disposal *in vivo* occurs through both insulin-dependent and insulin-independent mechanism [32]. We observed that treatment of SGR, FGR and the control Huh-7.5 cells with insulin (10^{-4} M to 10^{-9} M) increased glucose uptake by only about 50% from their basal levels (data not shown). Nevertheless, decreased glucose uptake by HCV-infected hepatocytes is a potential cause of hyperglycemia as the liver is a big organ accounting for 2% of the total body weight.

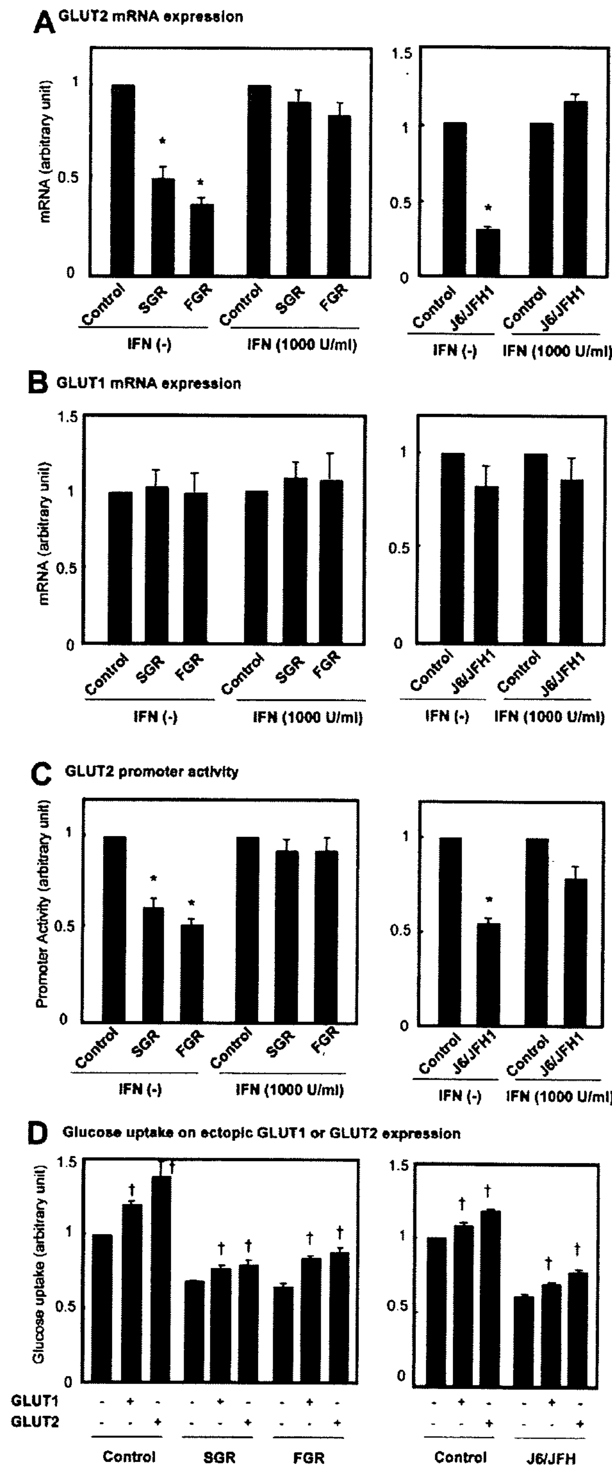

Fig. 6. Differential suppression of GLUT2 and GLUT1 mRNAs by HCV replication. (A and B) Quantitative RT-PCR analysis of mRNA for GLUT2 (A) and GLUT1 (B). mRNA expression levels of GLUT2 and GLUT1 in SGR, FGR and HCV-infected cells were determined and normalized with β-glucuronidase mRNA levels. In parallel, cells were treated with IFN (1000 IU/ml) for 10 days to eliminate HCV replication before being subjected to quantitative RT-PCR analysis. Data represent mean ± SEM of three independent experiments. $^{*}P < 0.01$, compared with the control. (C) GLUT2 promoter activities in SGR and FGR, HCV-infected cells were analyzed using luciferase reporter assay. In parallel, cells were treated with IFN (1000 IU/ml) for 10 days to eliminate HCV replication before being subjected to luciferase reporter assay. Data represent mean ± SEM of five independent experiments. $^{*}P < 0.01$, compared with the control. (D) Glucose uptake in cells ectopically expressing GLUT1 or GLUT2. Data represent mean ± SEM of two independent experiments. $^{\dagger}P < 0.01$, compared with mock transfected control.

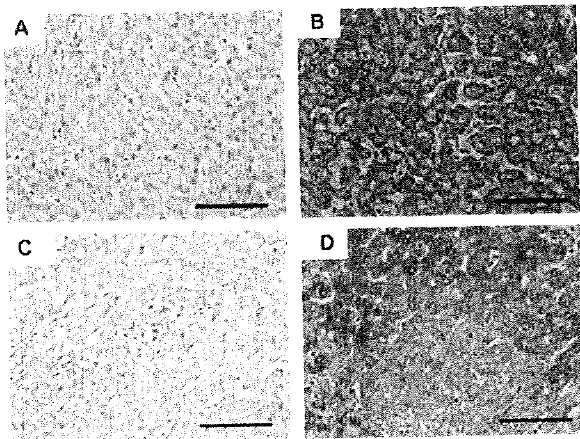

Fig. 7. Down-regulation of GLUT2 expression in HCV-infected human liver tissues *in vivo*. Normal human adult liver tissues (A and B) and HCV-infected, non-cancerous liver tissues (C and D) were fixed with formalin, sectioned and stained with normal rabbit IgG (A and C) or polyclonal anti-GLUT2 antibody (B and D). Scale bar = 100 μm.

Any proliferating cell requires energy sources, including glucose, and GLUTs play an important role in glucose uptake into the cell. In the liver, GLUT2 is the predominant glucose transporter, which regulates glucose metabolism by mediating a bidirectional transport, both entry and exit, of glucose into and from hepatocytes [13]. GLUT1, on the other hand, is known to be

Table 2
Reduction of GLUT2 expression in hepatocytes of HCV-infected and HBV-infected human liver tissues.

Liver tissues	Sample No.	Reduction of GLUT2 expression
Uninfected	1	– *
	2	–
	3	–
	4	–
	5	–
	6	–
	7	–
	8	–
HCV-infected	9	1+ (Focal)[a]
	10	1+ (Focal)
	11	3+ (Diffuse)
	12	3+ (Diffuse)
	13	3+ (Diffuse)
	14	3+ (Focal)
	15	–
	16	2+ (Focal)
	17	3+ (Diffuse)
HBV-infected	18	–
	19	3+ (Diffuse)
	20	1+ (Focal)
	21	–
	22	2+ (Focal)
	23	1+ (Focal)
	24	2+ (Focal)

* -, no reduction; 1+, weak reduction; 2+, moderate reduction; 3+, strong reduction.
[a] Parentheses indicate either focal or diffuse appearance of the areas with reduced GLUT2 expression in each liver tissue sample.

expressed in malignant cells including hepatocellular carcinoma [12,13] and a wide variety of cultured cells. In the present study we found that cell surface expression of GLUT2 and GLUT1 was markedly suppressed in SGR, FGR and HCV-infected cells compared to the control (Fig. 4A and B).

GLUT2 expression is regulated at the transcriptional level, at least partly, by glucose [33]. It has been reported that hyperglycemia increases the GLUT2 mRNA and protein expression in an *in vivo* study [34]. Our present study demonstrated that GLUT2 mRNA expression was significantly suppressed in SGR, FGR and HCV-infected cells compared to the control (Fig. 6A). Consistent with this result, GLUT2 promoter activities, as measured by luciferase reporter assay, were suppressed in SGR, FGR and HCV-infected cells (Fig. 6C). In this connection, it was reported that GLUT2 promoter activities were up-regulated by sterol response element-binding protein (SREBP)-1c [35,36]. We confirmed in our study that GLUT2 promoter activities were up-regulated by over-expression of human SREBP-1c, and that the SREBP-1c-mediated GLUT2 promoter activities were suppressed significantly in SGR, FGR and HCV-infected cells (data not shown).

Unlike GLUT2 mRNA, GLUT1 mRNA was not suppressed by HCV RNA replication or HCV infection (Fig. 6B). Nevertheless, cell surface expression of GLUT1 was markedly down-regulated in SGR and FGR cells (Fig. 4A). As GLUT1 surface expression was not restored by treatment with lactacystin, a potent proteasome inhibitor (Fig. 5), it was unlikely that HCV-mediated suppression of GLUT1 surface expression was mediated through increased degradation by the ubiquitin-proteasome system. We assume that intracellular trafficking of GLUT1 (and possibly GLUT2 as well) is impaired by HCV RNA replication although we could not precisely prove it due mainly to the lack of an appropriate antibody that enables us to monitor GLUT1 trafficking. Further study is needed to elucidate the issue.

By means of immunohistochemical analysis, we confirmed that GLUT2 was strongly expressed in hepatocytes of the liver tissues obtained from all of 8 individuals without HCV infection (Fig. 7B and Table 2). More importantly, we demonstrated that GLUT2 expression was significantly down-regulated in hepatocytes obtained from 8 of 9 HCV-infected patients (Fig. 7D and Table 2). Interestingly, the areas where GLUT2 down-regulation was observed appeared to be scattered across the liver tissue sections. This may reflect the general observation that a group of hepatocytes in limited areas of the hepatic lobules, but not all the hepatocytes, are infected with HCV *in vivo*. By means of real-time quantitative PCR analysis, we found a tendency that levels of GLUT2 mRNA expression in liver tissues obtained from HCV-infected patients were lower than that obtained from uninfected controls although the dif-

ference was not statistically significant (data not shown). As stated above, not all the hepatocytes in the liver were infected with HCV and, therefore, the possible reduction of GLUT2 mRNA expression in HCV-infected hepatocytes might have been masked by the normal levels of expression in uninfected hepatocytes concomitantly present in the same tissue samples.

It should also be noted that GLUT2 staining was also reduced in hepatocytes obtained from HBV-infected patients, though to a lesser extent than that from HCV-infected ones (Table 2). We assume that inflammatory responses in the liver may trigger some intracellular event that leads to decreased GLUT2 expression in hepatocytes *in vivo*.

In conclusion, we have demonstrated for the first time that HCV replication inhibits cellular glucose uptake through down-regulation of cell surface expression of GLUT2 and possibly GLUT1. It is conceivable that the decreased glucose uptake by hepatocytes causes impaired glucose metabolism, leading eventually to the initiation and progression of diabetes mellitus during a prolonged period of HCV persistence.

Acknowledgements

The authors are grateful to Dr. C.M. Rice (The Rockefeller University, New York, NY, USA) for providing pFL-J6/JFH1 and Huh7.5 cells. Thanks are also due to Dr. R. Bartenschlager (University of Heidelberg, Heidelberg, Germany) for providing an HCV subgenomic RNA replicon (pFK5B/2884Gly) and Dr. R. Sato (The University of Tokyo, Tokyo, Japan) for providing a human SREBP-1c expression plasmid (pME-hSREBP-1c). This study was supported in part by grants-in-aid for Scientific Research from the Ministry of Education, Culture, Sports, Science and Technology (MEXT) and the Ministry of Health, Labour and Welfare, Japan. This study was also carried out as part of the Program of Founding Research Centers for Emerging and Reemerging Infectious Diseases, MEXT, Japan, and the Global Center of Excellence (COE) Program at Kobe University Graduate School of Medicine.

Appendix A. Supplementary data

Supplementary data associated with this article can be found, in the online version, at doi:10.1016/j.jhep.2008.12.029.

References

[1] Simmonds P, Bukh J, Combet C, Deléage G, Enomoto N, Feinstone S, et al. Consensus proposals for a unified system of nomenclature of hepatitis C virus genotypes. Hepatology 2005;42:962–973.

[2] Lu L, Li C, Fu Y, Thaikruea L, Thongswat S, Maneekarn N, et al. Complete genomes for hepatitis C virus subtypes 6f, 6i, 6j and 6m: viral genetic diversity among Thai blood donors and infected spouses. J Gen Virol 2007;88:1505–1518.

[3] Lindenbach BD, Rice CM. Unravelling hepatitis C virus replication from genome to function. Nature 2005;436:933–938.

[4] Appel N, Schaller T, Penin F, Bartenschlager R. From structure to function: new insights into hepatitis C virus RNA replication. J Biol Chem 2006;281:9833–9836.

[5] Shepard CW, Finelli L, Alter MJ. Global epidemiology of hepatitis C virus infection. Lancet Infect Dis 2005;5:558–567.

[6] Galossi A, Guarisco R, Bellis L, Puoti C. Extrahepatic manifestations of chronic HCV infection. J Gastrointestin Liver Dis 2007;16:65–73.

[7] Caronia S, Taylor K, Pagliaro L, Carr C, Palazzo U, Petrik J, et al. Further evidence for an association between non-insulin-dependent diabetes mellitus and chronic hepatitis C virus infection. Hepatology 1999;30:1059–1063.

[8] Mason AL, Lau JY, Hoang N, Qian K, Alexander GJ, Xu L, et al. Association of diabetes mellitus and chronic hepatitis C virus infection. Hepatology 1999;29:328–333.

[9] Mehta S, Levey JM, Bonkovsky HL. Extrahepatic manifestations of infection with hepatitis C virus. Clin Liver Dis 2001;5:979–1008.

[10] Mehta SH, Brancati FL, Sulkowski MS, Strathdee SA, Szklo M, Thomas DL. Prevalence of type 2 diabetes mellitus among persons with hepatitis C virus infection in the United States. Ann Intern Med 2000;133:592–599.

[11] Wu X, Freeze HH. GLUT14, a duplicon of GLUT3, is specifically expressed in testis as alternative spice forms. Genomics 2002;80:553–557.

[12] Macheda ML, Rogers S, Best JD. Molecular and cellular regulation of glucose transporter (GLUT) proteins in cancer. J Cell Physiol 2005;202:654–662.

[13] Godoy A, Ulloa V, Rodriguez F, Reinicke K, Yanez AJ, Garcia Mde L, et al. Differential subcellular distribution of glucose transporters GLUT1-6 and GLUT9 in human cancer: ultrastructural localization of GLUT1 and GLUT5 in breast tumor tissues. J Cell Physiol 2006;207:614–627.

[14] Ban N, Yamada Y, Someya Y, Miyawaki K, Ihara Y, Hosokawa M, et al. Hepatocyte nuclear factor-1α recruits the transcriptional co-activator p300 on the GLUT2 gene promoter. Diabetes 2002;51:1409–1418.

[15] Blight KJ, McKeating JA, Rice CM. Highly permissive cell lines for subgenomic and genomic hepatitis C virus RNA replication. J Virol 2002;76:13001–13014.

[16] Hidajat R, Nagano-Fujii M, Deng L, Tanaka M, Takigawa Y, Kitazawa S, et al. Hepatitis C virus NS3 protein interacts with ELKS-δ and ELKS-α, members of a novel protein family involved in intracellular transport and secretory pathways. J Gen Virol 2005;86:2197–2208.

[17] Nomura-Takigawa Y, Nagano-Fujii M, Deng L, Kitazawa S, Ishido S, Sada K, et al. Non-structural protein 4A of Hepatitis C virus accumulates on mitochondria and renders the cells prone to undergoing mitochondria-mediated apoptosis. J Gen Virol 2006;87:1935–1945.

[18] Inubushi S, Nagano-Fujii M, Kitayama K, Tanaka M, An C, Yokozaki H, et al. Hepatitis C virus NS5A protein interacts with and negatively regulates the non-receptor protein-tyrosine kinase Syk. J Gen Virol 2008;89:1231–1242.

[19] Ikeda M, Abe K, Dansako H, Nakamura T, Naka K, Kato N. Efficient replication of a full-length hepatitis C virus genome, strain O, in cell culture, and development of a luciferase reporter system. Biochem Biophys Res Commun 2005;329:1350–1359.

[20] Deng L, Nagano-Fujii M, Tanaka M, Nomura-Takigawa Y, Ikeda M, Kato N, et al. NS3 protein of Hepatitis C virus associates with the tumour suppressor p53 and inhibits its

function in an NS3 sequence-dependent manner. J Gen Virol 2006;87:1703–1713.

[21] Lindenbach BD, Evans MJ, Syder AJ, Wolk B, Tellinghuisen TL, Liu CC, et al. Complete replication of hepatitis C virus in cell culture. Science 2005;309:623–626.

[22] Deng L, Adachi T, Kitayama K, Bungyoku Y, Kitazawa S, Ishido S, et al. Hepatitis C virus infection induces apoptosis through a Bax-triggered, mitochondrion-mediated, caspase 3-dependent pathway. J Virol 2008;82:10375–10385.

[23] Kanda H, Tamori Y, Shinoda H, Yoshikawa M, Sakaue M, Udagawa J, et al. Adipocytes from Munc18c-null mice show increased sensitivity to insulin-stimulated GLUT4 externalization. J Clin Invest 2005;115:291–301.

[24] Niwa H, Yamamura K, Miyazaki J. Efficient selection for high-expression transfectants with a novel eukaryotic vector. Gene 1991;108:193–199.

[25] Lehner PJ, Hoer S, Dodd R, Duncan LM. Downregulation of cell surface receptors by the K3 family of viral and cellular ubiquitin E3 ligase. Immunol Rev 2005;207:112–125.

[26] Mehta SH, Brancati FL, Strathdee SA, Pankow JS, Netski D, Coresh J, et al. Hepatitis C virus infection and incident type 2 diabetes. Hepatology 2003;38:50–56.

[27] Wang CS, Wang ST, Yao WJ, Chang TT, Chou P. Hepatitis C virus infection and the development of type 2 diabetes in a community-based longitudinal study. Am J Epidemiol 2007;166:196–203.

[28] Hui JM, Sud A, Farrell GC, Bandara P, Byth K, Kench JG, et al. Insulin resistance is associated with chronic hepatitis C virus infection and fibrosis progression. Gastroenterology 2003;125:1695–1704.

[29] Kawaguchi T, Yoshida T, Harada M, Hisamoto T, Nagao Y, Ide T, et al. Hepatitis C virus down-regulates insulin receptor substrates 1 and 2 through up-regulation of suppressor of cytokine signaling 3. Am J Pathol 2004;165:1499–1508.

[30] Miyamoto H, Moriishi K, Moriya K, Murata S, Tanaka K, Suzuki T, et al. Involvement of the PA28γ-dependent pathway in insulin resistance induced by hepatitis C virus core protein. J Virol 2007;81:1727–1735.

[31] Ader M, Ni TC, Bergman RN. Glucose effectiveness assessed under dynamic and steady state conditions. Comparability of uptake versus production components. J Clin Invest 1997;99:1187–1199.

[32] Banerjee S, Saito K, Ait-Goughoulte M, Meyer K, Ray RB, Ray R. Hepatitis C virus core protein upregulates serine phosphorylation of IRS-1 and impairs downstream Akt/PKB signaling pathway for insulin resistance. J Virol 2008;82:2606–2612.

[33] Im SS, Kim SY, Kim HI, Ahn YH. Transcriptional regulation of glucose sensors in pancreatic beta cells and liver. Curr Diabetes Rev 2006;2:11–18.

[34] Adachi T, Yasuda K, Okamoto Y, Shihara N, Oku A, Ueta K, et al. T-1095, a renal Na^+-glucose transporter inhibitor, improves hyperglycemia in streptozotocin-induced diabetic rats. Metabolism 2000;49:990–995.

[35] Im SS, Kang SY, Kim SY, Kim HI, Kim JW, Kim KS, et al. Glucose-stimulated upregulation of GLUT2 gene is mediated by sterol response element-binding protein-1c in the hepatocytes. Diabetes 2005;54:1684–1691.

[36] Kanayama T, Arito M, So K, Hachimura S, Inoue J, Sato R. Interaction between sterol regulatory element-binding proteins and liver receptor homolog-1 reciprocally suppresses their transcriptional activities. J Biol Chem 2007;282:10290–10298.

 DOI 10.1099/vir.0.010983-0

Efficient production of infectious hepatitis C virus with adaptive mutations in cultured hepatoma cells

Yasuaki Bungyoku, Ikuo Shoji, Tatsuhiko Makine, Tetsuya Adachi, Kazumi Hayashida, Motoko Nagano-Fujii, Yoshi-Hiro Ide, Lin Deng and Hak Hotta

Correspondence
Hak Hotta
hotta@med.kobe-u.ac.jp

Division of Microbiology, Kobe University Graduate School of Medicine, 7-5-1 Kusunoki-cho, Chuo-ku, Kobe, Hyogo 650-0017, Japan

Robust production of infectious hepatitis C virus (HCV) in cell culture was realized by using the JFH1 strain and the homologous chimeric J6/JFH1 strain in Huh-7.5 cells, a highly HCV-permissive subclone of Huh-7 cells. In this study, we aimed to establish a more efficient HCV-production system and to gain some insight into the adaptation mechanisms of efficient HCV production. By serial passaging of J6/JFH1-infected Huh-7.5 cells, we obtained culture-adapted J6/JFH1 variants, designated P-27, P-38 and P-47. Sequence analyses revealed that the adaptive mutant viruses P-27, P-38 and P-47 possessed eight mutations [four in E2, two in NS2, one in NS5A and one in NS5B), 10 mutations [two additional mutations in the 5′-untranslated region (5′-UTR) and core] and 11 mutations (three additional mutations in 5′-UTR, core and NS5B), respectively. We introduced amino acid substitutions into the wild-type J6/JFH1 clone, generated recombinant viruses with adaptive mutations and analysed their infectivity and ability to produce infectious viruses. The viruses with the adaptive mutations exhibited higher expression of HCV proteins than did the wild type in Huh-7.5 cells. Moreover, we provide evidence suggesting that the mutation N534H in the E2 glycoprotein of the mutant viruses conferred an advantage at the entry level. We thus demonstrate that an efficient HCV-production system could be obtained by introducing adaptive mutations into the J6/JFH1 genome. The J6/JFH1-derived mutant viruses presented here would be a good tool for producing HCV particles with enhanced infectivity and for studying the molecular mechanism of HCV entry.

Received 11 February 2009
Accepted 5 March 2009

INTRODUCTION

Hepatitis C virus (HCV) is the main cause of chronic hepatitis, liver cirrhosis and hepatocellular carcinoma (Choo *et al.*, 1989; Kuo *et al.*, 1989; Saito *et al.*, 1990). As more than 170 million people worldwide are infected chronically with HCV (Poynard *et al.*, 2003) and because the current antiviral therapy, interferon and ribavirin, produces sustained virus clearance in <50 % of treated patients (Manns *et al.*, 2007), HCV infection is clearly a problem of major proportions. HCV is a single-stranded, positive-sense RNA virus that is classified in the genus *Hepacivirus* in the family *Flaviviridae*. The approximately 9.6 kb HCV genome encodes one large open reading frame (ORF) that is flanked at the 5′ and 3′ ends by untranslated regions (UTRs) (Choo *et al.*, 1991). The HCV polyprotein is processed into at least 10 proteins by viral proteases and cellular signalases (Grakoui *et al.*, 1993; Hijikata *et al.*, 1993a; McLauchlan *et al.*, 2002). The structural proteins core, E1 and E2 are located in the N terminus of the polyprotein, followed by p7 and the non-structural (NS) proteins NS2, NS3, NS4A, NS4B, NS5A and NS5B (Bartenschlager & Sparacio, 2007).

Study of the HCV life cycle and virus–host interaction has been hampered severely by the lack of a robust *in vitro* cell-culture system and small-animal models of HCV infection (Bartenschlager & Sparacio, 2007). The development of HCV replicon systems has made an important contribution to the study of HCV translation and RNA replication in the human hepatoma cell line Huh-7 (Blight *et al.*, 2000; Lohmann *et al.*, 1999). Sequence analyses of multiple HCV replicons have revealed that several adaptive mutations enhance RNA replication to varying degrees (Bartenschlager & Sparacio, 2007; Blight *et al.*, 2000; Lohmann *et al.*, 2001). Such adaptive mutations were primarily identified in a central portion of the NS5A protein. Although the extent to which these adaptive mutations enhance RNA replication was subsequently studied by using various transient replication assays, the molecular mechanism underlying replication enhancement still remains elusive (Bartenschlager & Sparacio, 2007). The HCV replicons containing adaptive mutations do not produce infectious virus particles in culture and are severely attenuated (Blight *et al.*, 2002; Pietschmann *et al.*, 2002). Using recombinant HCV envelope glycoproteins

010983 © 2009 SGM

and HCV pseudoparticles, several cell-surface molecules have been shown to interact with HCV during virus binding and entry, including the tetraspanin CD81 (Bartosch *et al.*, 2003; Pileri *et al.*, 1998), the scavenger receptor class B member I (SR-BI) (Bartosch *et al.*, 2003; Scarselli *et al.*, 2002) and the tight junction protein claudin-1 (CLDN1) (Evans *et al.*, 2007).

The major breakthrough was made by establishing an HCV-production system using HCV strain JFH1, a genotype 2a isolate, and Huh-7 cells (Wakita *et al.*, 2005). Two other groups reported a robust production of infectious virus using a homologous chimeric FL-J6/JFH1 strain (Lindenbach *et al.*, 2005) or using Huh-7.5.1 cells (Zhong *et al.*, 2005) derived from the cell line Huh-7.5, which has a defect in the RIG-I pathway (Sumpter *et al.*, 2005). Upon transfection of Huh-7 cells with the *in vitro*-transcribed HCV JFH1 genome or the chimera FL-J6/JFH1, infectious HCV particles were secreted in an envelope glycoprotein-dependent manner (Lindenbach *et al.*, 2005; Wakita *et al.*, 2005; Zhong *et al.*, 2005). Using HCV-production systems, adaptive or compensatory mutations that promote the production of infectious virus from wild-type JFH1 (Delgrange *et al.*, 2007; Kaul *et al.*, 2007; Russell *et al.*, 2008; Zhong *et al.*, 2006) or chimeric viruses (Gottwein *et al.*, 2007; Yi *et al.*, 2006, 2007) have been identified. However, the molecular mechanisms of adaptive mutations are poorly understood.

In this study, we aimed to establish an efficient HCV-production system and to gain more insight into the determinants of efficient virus production. By serial passaging of Huh-7.5 cells infected with the HCV J6/JFH1 strain, we identified adaptive mutations in the clones and analysed the mutations by examining the production of the recombinant mutant viruses.

METHODS

Cell culture. Huh-7.5 cells (Blight *et al.*, 2002), a highly HCV-permissive subclone of Huh-7 cells, were kindly provided by Dr C. M. Rice (Rockefeller University, New York, NY, USA). Cells were cultured in Dulbecco's modified Eagle's medium (DMEM; Wako) supplemented with 10 % fetal bovine serum (FBS; Biowest), 0.1 mM non-essential amino acids (Invitrogen), 100 IU penicillin ml^{-1} and 100 µg streptomycin ml^{-1} (Invitrogen). DMEM containing 10 % FBS was designated complete DMEM. Cells were grown at 37 °C in a CO_2 incubator.

Antibodies. The mouse monoclonal antibodies (mAbs) used in this study were anti-core (2H9) mAb (Wakita *et al.*, 2005) and anti-HCV NS3 mAb (Chemicon). Goat anti-actin polyclonal antibody (C-11) (Santa Cruz Biotech) was used. Horseradish peroxidase (HRP)-conjugated goat anti-mouse IgG (MBL) and HRP-conjugated donkey anti-goat IgG (Santa Cruz Biotech) were used as secondary antibodies.

Plasmids. Plasmid pFL-J6/JFH1 (Lindenbach *et al.*, 2005) containing the full-length chimeric HCV genome was used to generate infectious HCV. Amino acid substitutions were introduced by site-directed mutagenesis using a QuikChange site-directed mutagenesis kit (Stratagene). All PCR-amplified DNA fragments were verified extensively by using an ABI PRISM 3100-Avant Genetic Analyzer (Applied Biosystems). The primer sequences used in this study are available from the authors upon request.

HCV RNA transfection and virus production. The pFL-J6/JFH1 plasmid was linearized with *Xba*I and *in vitro*-transcribed by using the T7 RiboMAX Express large-scale RNA production system (Promega) following the manufacturer's instructions. The quality of synthesized RNA was examined by agarose gel electrophoresis. Cells were trypsinized and washed with serum-free DMEM. In total, 6×10^6 cells were suspended in 500 µl serum-free DMEM and mixed with 10 µg *in vitro*-transcribed RNA in a 4 mm cuvette (Bio-Rad). The synthesized RNA was introduced into Huh-7.5 cells by electroporation using a Bio-Rad Gene Pulser system with a single pulse at 270 V, 975 µF. The cells were then plated in 10 cm culture dishes containing complete DMEM.

Indirect immunofluorescence. Immunofluorescence staining was performed essentially as described previously (Takigawa *et al.*, 2004). Cells seeded on glass coverslips in a 24-well plate at a density of 4×10^4 cells per well were infected with HCV. Cells were cultured, washed with PBS and fixed with 3.7 % paraformaldehyde in PBS for 10 min at room temperature, followed by permeabilization in 0.1 % Triton X-100 in PBS for 10 min at room temperature. After being washed twice with PBS, cells were blocked with 5 % goat serum in PBS and then incubated with the serum of an HCV-infected patient with a high titre of anti-HCV antibodies. Fluorescein isothiocyanate-conjugated goat anti-human IgG (MBL) was used as a secondary antibody. The cells were washed with PBS, counterstained with Hoechst 33342 solution (Molecular Probes) at room temperature for 10 min, mounted on glass slides and examined under a fluorescence microscope (BX51; Olympus).

Virus titration. Culture supernatants were diluted serially 10-fold in complete DMEM and used to infect 2×10^5 naïve Huh-7.5 cells per well in 24-well plates. The inoculum was incubated with cells for 6 h at 37 °C and then supplemented with fresh complete DMEM. The level of HCV infection was determined 1 day post-infection by immunofluorescence using anti-HCV polyclonal antibody. The virus titre was expressed in focus-forming units (ml supernatant)$^{-1}$ (f.f.u. ml^{-1}), as determined by the mean number of HCV-positive foci detected at the highest dilutions according to a previously described method (Zhong *et al.*, 2005).

Immunoblotting. Immunoblotting was performed essentially as described previously (Muramatsu *et al.*, 1997). To detect the expression of HCV proteins, the immune complexes were visualized by an ECL Western blotting detection kit (GE Healthcare) following the manufacturer's instructions.

HCV RNA quantification. Total RNA was extracted by using RNAiso (TaKaRa) according to the manufacturer's instructions. One microgram of isolated RNA was reverse-transcribed by using a QuantiTect reverse transcription kit (Qiagen) with random primers. RT-qPCR analysis was performed as described previously (Zhong *et al.*, 2005). HCV RNA was monitored by using the PCR primers 5′-TCTGCGGAACCGGTGAGTA-3′ (sense) and 5′-TCAGGCAGTA-CCACAAGGC-3′ (antisense). HCV transcript levels were determined relative to a standard curve comprising serial dilutions of plasmid containing the HCV J6/JFH1 cDNA.

HCV RNA genome sequencing. HCV RNA was isolated from 140 µl viral supernatant by using a QIAamp Viral RNA Mini kit (Qiagen), and then used as a template to generate cDNA in a reverse-transcription reaction using SuperScript One-Step RT-PCR with Platinum *Taq* (Invitrogen) according to the manufacturer's instruc-

tions. PCR primers of between 20 and 26 bases, designed using the sequence of J6/JFH1, were used to amplify four fragments of HCV cDNA (nt 49–3517, 2582–5966, 5832–8038 and 7870–9286) to cover most of the HCV genome. In addition, the 5′-end sequence was amplified by using the 5′ RACE System for Rapid Amplification of cDNA Ends (Invitrogen) and the 3′-end sequence was amplified by using a 3′-Full RACE Core set (TaKaRa). The sequences of the amplified DNA were determined by using an ABI PRISM 3100-Avant Genetic Analyzer.

Quantification of HCV core protein. HCV core protein in the cells or cell-culture supernatants was quantified by using a highly sensitive enzyme immunoassay (Ortho HCV antigen ELISA kit; Ortho Clinical Diagnostics). To determine intracellular amounts of core, cell lysates were prepared as described by Schaller *et al.* (2007).

Blocking of virus attachment and entry with anti-CD81 antibody. Blocking of virus attachment and entry with anti-CD81 antibody was performed essentially as described previously (Wakita *et al.*, 2005). Huh-7.5 cells (6×10^4 cells per 24-well plate) were pretreated with anti-CD81 antibody (clone JS-81; BD Biosciences) or an isotype-matched control antibody (purified mouse IgG1, κ isotype control; BD Biosciences) as indicated for 1 h. Cells were then infected with the wild-type or mutant viruses at an m.o.i. of 0.5 or 0.01 for 6 h. The viruses were removed, and the cells were washed with PBS and then supplemented with complete DMEM. The efficiency of infection was monitored 1 day after infection by counting the number of HCV-positive foci by immunofluorescence.

Statistical analysis. A two-tailed Student's *t*-test was applied to evaluate the statistical significance of differences measured from the datasets. A P value of <0.05 was considered to be statistically significant.

RESULTS

Increase in HCV infectivity titres during serial passage

To produce infectious HCV particles, *in vitro*-transcribed genomic J6/JFH1 RNA was electroporated into Huh-7.5 cells. Transfected Huh-7.5 cells were maintained and the infectivity titre of the culture supernatant reached 6×10^4 f.f.u. ml^{-1} at 20 days post-infection. This culture supernatant was designated P-1.

To generate higher infectivity titres for HCV, naïve Huh-7.5 cells (3×10^5 cells per six-well plate) were infected with 1 ml virus stock of P-1 (6×10^4 f.f.u. ml^{-1}) at an m.o.i. of 0.2 and the infected cells were passaged serially every 3–4 days to maintain a subconfluent culture for 6 months. The culture medium was replaced with fresh complete DMEM every day. The extracellular infectivity titres fluctuated in the beginning after transfection and became lowest at the 22nd passage (Fig. 1a). Thereafter, the extracellular infectivity titres increased again and reached highest infectivity at the 47th passage. Therefore, we further examined the supernatants at the 27th, 38th and 47th passages, and the viruses were designated P-27, P-38 and P-47, respectively. The infectivity titres were determined to be 7.0×10^3 f.f.u. ml^{-1} for P-27, 1.7×10^4 f.f.u. ml^{-1} for P-38 and 3.3×10^4 f.f.u. ml^{-1} for P-47 (Fig. 1a). These viruses were used as inocula in the following experiments.

Kinetics of virus production after infection with putative adaptive J6/JFH1 mutants

To examine the virus-production kinetics of these viruses in Huh-7.5 cells, naïve Huh-7.5 cells (3×10^4 cells per 24-well plate) were infected with each inoculum (6×10^3 f.f.u.) at an m.o.i. of 0.2. After infection, the culture supernatants were harvested each day for 10 days and assayed for infectivity titres (Fig. 1b). The P-1 virus showed a peak infectivity titre of 2.3×10^4 f.f.u. ml^{-1} at 4 days post-infection, whereas the P-27, P-38 and P-47 viruses showed peak titres of 1.0×10^6, 2.3×10^6 and 6.0×10^6 f.f.u. ml^{-1} at 4–5 days post-infection, respectively (Fig. 1b), suggesting that these three viruses produce infectious HCV particles more efficiently than the P-1 virus. The increased infectivity titres may have been due to an increase in the absolute number of released HCV particles or an increased proportion of infectious relative to non-infectious particles. To address this question, we compared the specific infectivities of the mutant viruses with those of the wild-type virus. The ratio of viral infectivity titre (f.f.u. ml^{-1}) to HCV RNA content [genome equivalents (GE) ml^{-1}] was determined as shown in Table 1. The mutant viruses, P-27, P-38 and P-47, had higher specific-infectivity titres (1 : 21, 1 : 10 and 1 : 10, respectively) than the wild-type virus P-1 (1 : 133), suggesting that the mutant viruses are more infectious than the wild type and that the mutant viruses possess adaptive mutations in the virus genomes.

Sequence analysis of genetic mutations in the adaptive mutants

To identify the genetic changes in the virus genomes that are responsible for the adaptation to Huh-7.5 cells, we sequenced the whole genomes of the viruses. No mutation was found in the P-1 virus, whereas several mutations were identified in the P-27, P-38 and P-47 viruses (Fig. 1c). The sequencing analysis of P-27 identified eight mutations that were located in the E2, NS2, NS5A and NS5B regions as follows: T396A, T416A, N534H and A712V in E2; Y852H and W879R in NS2; F2281L in NS5A; and M2876L in NS5B (Fig. 1c). P-38 possessed 10 mutations, the same mutations as in P-27 and two additional mutations. The additional mutations were found at nucleotide position 146 (U to A) in the 5′-UTR and an amino acid change, K78E, in the core region. P-47 contained 11 mutations, including the same 10 mutations as P-38 and one additional mutation, T2925A in NS5B. Thus, the first eight mutations were all present in the genomes of the three viruses, and the results suggested that these eight mutations contribute to the enhanced infectivity.

Effects of individual mutations on the production of infectious HCV

To determine which mutation is responsible for the enhancement of infectivity, recombinant genomes containing only one of the selected mutations were constructed

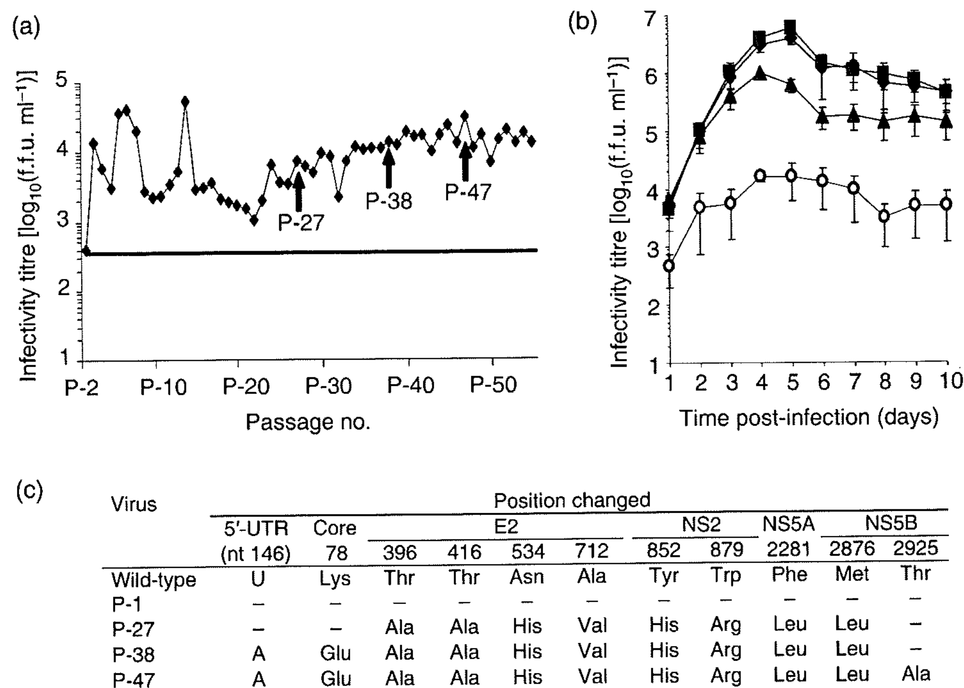

Virus	Position changed										
	5′-UTR	Core	E2				NS2		NS5A	NS5B	
	(nt 146)	78	396	416	534	712	852	879	2281	2876	2925
Wild-type	U	Lys	Thr	Thr	Asn	Ala	Tyr	Trp	Phe	Met	Thr
P-1	–	–	–	–	–	–	–	–	–	–	–
P-27	–	–	Ala	Ala	His	Val	His	Arg	Leu	Leu	–
P-38	A	Glu	Ala	Ala	His	Val	His	Arg	Leu	Leu	–
P-47	A	Glu	Ala	Ala	His	Val	His	Arg	Leu	Leu	Ala

Fig. 1. Increase in HCV infectivity titres during serial passage. (a) Serial passage of HCV J6/JFH1-infected Huh-7.5 cells. Huh-7.5 cells (3×10^5 cells per six-well plate) were infected with 1 ml stock of wild-type J6/JFH1 virus (P-1) (6×10^4 f.f.u. ml^{-1}) at an m.o.i. of 0.2, and the infected cells were passaged serially every 3–4 days to maintain a subconfluent culture for 6 months. The culture medium was replaced with fresh complete DMEM each day. The extracellular infectivity titres were determined by titration assay and are expressed as f.f.u. ml^{-1}. Arrows show the time points at which we collected the putative adapted viruses, designated P-27, P-38 and P-47. (b) Kinetics of virus production after infection with putative J6/JFH1 adaptive mutants in Huh-7.5 cells. Huh-7.5 cells were infected with the wild-type J6/JFH1 virus (○, P-1) or putative adaptive mutants (▲, P-27; ◆, P-38; ■, P-47) at an m.o.i. of 0.2. After infection, the culture supernatants were harvested every day until 10 days post-infection. Infectivity titres were measured by immunofluorescence assay and are expressed as f.f.u. ml^{-1}. Error bars represent SD for triplicate measurements. (c) Genetic mutations identified during passage. Numbers indicate the amino acid position where mutations were identified. The nucleotide position with mutation is given in parentheses.

(Fig. 2a). The *in vitro*-transcribed mutant J6/JFH1 RNAs were electroporated into Huh-7.5 cells and mutant viruses were generated. Then, naïve Huh-7.5 cells were infected with each virus at an m.o.i. of 0.01 and cultured for 12 days. The culture supernatant was collected every day from 1 to 12 days post-infection. The ability of each mutant virus to release infectious virus particles was examined by titration assay. As shown in Fig. 2(b), the recombinant viruses with single point mutations did not enhance the production of infectious virus particles, suggesting that a single point mutation is not enough for the enhanced infectivity.

Table 1. Specific-infectivity titres of the adaptive J6/JFH1 mutant viruses

Virus	HCV RNA copies [log$_{10}$(GE ml^{-1})]	Infectivity titre [log$_{10}$(f.f.u. ml^{-1})]	Specific infectivity (f.f.u. : GE)
P-1	6.7 ± 0.1	4.6 ± 0.1	1 : 133
P-27	7.3 ± 0.1	6.0 ± 0.2	1 : 21
P-38	7.4 ± 0.1	6.4 ± 0.0	1 : 10
P-47	7.3 ± 0.1	6.3 ± 0.2	1 : 10

Effects of combination of adaptive mutations on the production of infectious HCV

We then generated recombinant viruses with several mutations, as shown in Fig. 3(a). Naïve Huh-7.5 cells were infected with each virus at an m.o.i. of 0.01 and cultured for 12 days. The culture supernatant was collected every day from 1 to 12 days post-infection. The ability of each mutant virus to release infectious virus particles was examined by titration assay. The R-27, R-38 and R-47 viruses reached higher titres than the wild type and other mutant viruses, suggesting that all of the mutations in E2, NS2, NS5A and NS5B were important for the enhancement of infectivity (Fig. 3b). To determine the specific infectivities of the mutant viruses, the ratio of the viral infectivity titre (f.f.u. ml^{-1}) to the HCV RNA content (GE